Superharmonic resonances in a strongly coupled cavity-atom system

Eyal Buks,[1] Chunqing Deng,[2,3,4] Jean-Luc F. X. Orgazzi,[2,4,5] Martin Otto,[2,3,4] and Adrian Lupascu[2,3,4]

[1]*Department of Electrical Engineering, Technion, Haifa 32000 Israel*

[2]*Institute for Quantum Computing, University of Waterloo, Waterloo, Ontario, Canada N2L 3G1*

[3]*Department of Physics and Astronomy, University of Waterloo, Waterloo, ON, Canada N2L 3G1*

[4]*Waterloo Institute for Nanotechnology, University of Waterloo, Waterloo, Ontario, Canada N2L 3G1*

[5]*Department of Electrical and Computer Engineering, University of Waterloo, Waterloo, Ontario, Canada N2L 3G1*

(Received 13 January 2016; revised manuscript received 19 May 2016; published 8 September 2016)

We study a system consisting of a superconducting flux qubit strongly coupled to a microwave cavity. The fundamental cavity mode is externally driven and the response is investigated in the weak nonlinear regime. We find that near the crossing point, at which the resonance frequencies of the cavity mode and qubit coincide, the sign of the Kerr coefficient changes, and consequently the type of nonlinear response changes from softening to hardening. Furthermore, the cavity response exhibits superharmonic resonances (SHR) when the ratio between the qubit frequency and the cavity fundamental mode frequency is tuned close to an integer value. The nonlinear response is characterized by the method of intermodulation and both signal and idler gains are measured. The experimental results are compared with theoretical predictions and good qualitative agreement is obtained. The SHRs have potential for applications in quantum amplification and generation of entangled states of light.

DOI: 10.1103/PhysRevA.94.033807

I. INTRODUCTION

Cavity quantum electrodynamics (CQED) [1] is the study of the interaction between photons confined in a cavity and atoms (natural or artificial). The interaction is commonly described by the Rabi or Jaynes-Cummings Hamiltonians [2], and it has been the subject of numerous theoretical and experimental investigations. An on-chip CQED system can be realized by integrating a Josephson qubit [3–5] (playing the role of an artificial atom) with a superconducting microwave resonator (cavity) [6–8]. Superconducting CQED systems have generated a fast growing interest due to the possibility of reaching the strong [7] and ultrastrong [9,10] coupling regimes, and due to potential applications in quantum information processing [4,11–13].

In this study we investigate the driven dynamics of a strongly interacting system composed of a superconducting flux qubit [15,16] and a coplanar waveguide (CPW) microwave cavity [9,14,17–21]. The nonlinear cavity response [22–39] is measured as a function of the magnetic flux that is applied to the qubit. At weak driving and when the ratio between the qubit frequency and the cavity fundamental mode frequency is tuned close to the value $\omega_a/\omega_c = 1$ the common Jaynes-Cummings resonance, which henceforth is referred to as the primary resonance, is observed. With stronger driving, however, and when the ratio ω_a/ω_c is tuned close to integer values larger than unity, SHRs appear in the measured response. Intermodulation (IMD) measurements are employed to characterize the nonlinear response [40–42]. The results are compared with the predictions of a theoretical model, which is based on linearization of the equations of motion that govern the dynamics of the CQED system under study.

The investigated device contains a CPW cavity weakly coupled to two ports that are used for performing microwave transmission measurements [see Fig. 1(a)]. Two persistent current flux qubits [15], consisting of a superconducting loop interrupted by four Josephson junctions [see Fig. 1(c)], are inductively coupled to the CPW resonator [see Fig. 1(b)]. In the current experiment, however, only one qubit significantly affects the cavity mode response, whereas the other one is made effectively decoupled by detuning its energy gap away from the mode frequency. A CPW line terminated by a low inductance shunt is used to send microwave pulses for coherent qubit control [see Fig. 1(b)]. The device is fabricated on a high resistivity silicon substrate, in a two-step process. In the first step, the resonator and the control lines are defined using optical lithography, evaporation of a 190-nm thick aluminum layer and liftoff. In the second step, a bilayer resist is patterned by electron-beam lithography. Subsequently, shadow evaporation of two aluminum layers, 40 nm and 65 nm thick, respectively, followed by liftoff define the qubit junctions.

The chip is enclosed inside a copper package, which is cooled by a dilution refrigerator to a temperature of $T = 23$ mK. Both passive and active shielding methods are employed to suppress magnetic field noise. While passive shielding is performed using a three-layer high permeability metal, an active magnetic field compensation system placed outside the cryostat is used to actively reduce low-frequency magnetic field noise. A set of superconducting coils is used to apply dc magnetic flux. Qubit state control, which is employed in order to measure the qubit longitudinal T_1 and transverse T_2 relaxation times, is performed using shaped microwave pulses. Attenuators and filters are installed at different cooling stages along the transmission lines for qubit control and readout. A detailed description of sample fabrication and experimental setup can be found in [14,18].

II. THEORY

The main theoretical results needed for analyzing the experimental findings are briefly described below (derivations are given in the appendixes). The circulating current states of the qubit are labeled as $|\circlearrowleft\rangle$ and $|\circlearrowright\rangle$. The coupling between the cavity mode and the qubit is described by the term $-g(A + A^\dagger)(|\circlearrowleft\rangle\langle\circlearrowleft| - |\circlearrowright\rangle\langle\circlearrowright|)$ in the system

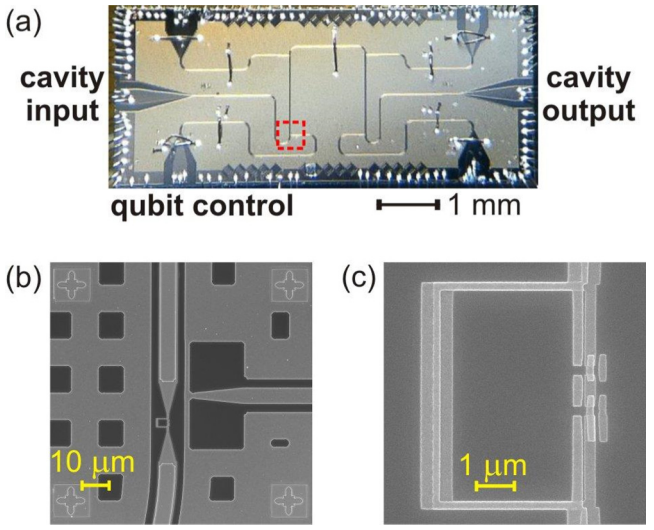

FIG. 1. The CQED device. (a) Optical image of the device, which is nominally identical to the one used in [14], where the overlaid dashed rectangle indicates the position of the qubit. (b) Electron micrograph showing a qubit embedded in the coplanar waveguide resonator and its local flux control line. (c) Electron micrograph of a flux qubit.

Hamiltonian, where A ($A^\dagger$) is a cavity mode annihilation (creation) operator, and g is the coupling coefficient. In the presence of an externally applied magnetic flux, the energy gap $\hbar\omega_a$ between the qubit ground state $|-\rangle$ and first excited state $|+\rangle$ is taken to be given by $\hbar\omega_a = \hbar\sqrt{\omega_f^2 + \omega_\Delta^2}$ [see Eq. (A7)], where

$$\omega_f = \frac{2I_{cc}\Phi_0}{\hbar}\left(\frac{\Phi_e}{\Phi_0} - \frac{1}{2}\right), \tag{1}$$

I_{cc} ($-I_{cc}$) is the circulating current associated with the state $|\curvearrowright\rangle$ ($|\curvearrowleft\rangle$), $\Phi_0 = h/2e$ is the flux quantum, Φ_e is the externally applied magnetic flux, and $\hbar\omega_\Delta$ is the qubit energy gap for the case where $\Phi_e/\Phi_0 = 1/2$.

The decoupled cavity mode is characterized by an angular resonance frequency ω_c, Kerr coefficient K_c, linear damping rate γ_c, and cubic damping (two-photon absorption) rate γ_{c4}. The response of the decoupled cavity in the weak nonlinear regime (in which, nonlinearity is taken into account to lowest nonvanishing order) can be described by introducing the complex and mode amplitude dependent cavity angular resonance frequency Υ_c, which is given by

$$\Upsilon_c = \omega_c - i\gamma_c + (K_c - i\gamma_{c4})E_c, \tag{2}$$

where E_c is the averaged number of photons occupying the cavity mode. The imaginary part of Υ_c represents the effect of damping and the terms proportional to E_c determine the weak nonlinear response. The effect of the flux qubit on the cavity response in the weak nonlinear regime is theoretically evaluated in Appendixes A and B for the case where $g/|\omega_c - \omega_a| \ll 1$. The coupling between the cavity mode and the qubit gives rise to a resonance splitting. The steady-state cavity mode response for the case where the qubit mainly occupies the state $|\pm\rangle$ (ground and first excited states) is found to be equivalent to the response of a mode having effective complex cavity angular resonance frequency Υ_{eff} given by

$$\Upsilon_{eff} = \Upsilon_c \pm \omega_{BS} \pm \Upsilon_{ba}, \tag{3}$$

where $\omega_{BS} = g_1^2/(\omega_c + \omega_a)$ is the Bloch-Siegert shift [10] [see Eq. (B15)]. The term Υ_{ba} is given by [see Eq. (A87)]

$$\Upsilon_{ba} = -\frac{g_1^2}{\Delta_1}\frac{1 - \frac{i}{\Delta_1 T_2}}{1 + \frac{1}{\Delta_1^2 T_2^2} + \frac{4g_1^2 T_1 E_c}{\Delta_1^2 T_2}}, \tag{4}$$

$g_1 = g/\beta_f$ is the flux dependent effective coupling coefficient, where the coefficient β_f is given by

$$\beta_f = \sqrt{1 + \left(\frac{\omega_f}{\omega_\Delta}\right)^2}, \tag{5}$$

and $\Delta_1 = \omega_p - \omega_a$ is the detuning between the angular frequency of the externally injected pump tone ω_p and the qubit angular resonance frequency ω_a. The expression (4) for Υ_{ba} is obtained by first deriving the equations of motion that govern the dynamics of the system [see Eqs. (A57), (A60), and (A62)]. In the next step the rotating wave approximation (RWA) is employed, and the resulting equations of motion [see Eqs. (A65), (A66), and (A67)] are linearized around fixed points [see Eqs. (A74), (A75), and (A76)]. In the last step the response of the system to external cavity driving is evaluated. Note that when $\Delta_1 T_2 \gg 1$ and when the qubit mainly occupies the state $|\pm\rangle$ the term Υ_{ba} gives rise to a shift in the mode angular frequency approximately given by $\mp g_1^2/\Delta_1$ and a shift in the value of the Kerr coefficient approximately given by $\pm(g_1^4/\Delta_1^3)(4T_1/T_2)$. Similar theoretical results have been obtained in Ref. [28], in which the unitary transformation that diagonalizes the Hamiltonian of the closed system has been applied to the system's master equation.

III. PRIMARY AND SUPERHARMONIC RESONANCES

The effect of the qubit on cavity response is experimentally investigated using transmission measurements. The color coded plots in Fig. 2 exhibit the measured [Figs. 2(a) and 2(c)] and calculated [Figs. 2(b) and 2(d)] cavity transmission (in dB units) vs $\omega_f/2\pi$, for the case where the power injected into the cavity is -127 dBm [Figs. 2(a) and 2(b)] and -112 dBm [Figs. 2(c) and 2(d)]. In the first step of the theoretical calculation, which has generated the theoretical predictions plotted in Figs. 2(b) and 2(d), fixed points are found by calculating steady-state solutions of the equations of motion that govern the dynamics of the system [see Eqs. (A81a), (A81b), and (A81c)]. Then in the second step input-output relations are employed in order to calculate the cavity transmission [see Eq. (A39)] [43]. The assumed device parameters are listed in the caption of Fig. 2. Note that intrinsic cavity mode nonlinearity is disregarded, i.e., it is assumed that $K_c = \gamma_{c4} = 0$, since the observed cavity nonlinearity is found to be dominated by back-reaction effects.

While the cavity response seen in Figs. 2(a) and 2(b) is nearly linear, nonlinearity [44] is observed in the results depicted in Figs. 2(c) and 2(d), which are obtained at higher input power (note the asymmetry in the resonance line shapes, i.e., cross sections of fixed ω_f). The measured response exhibits

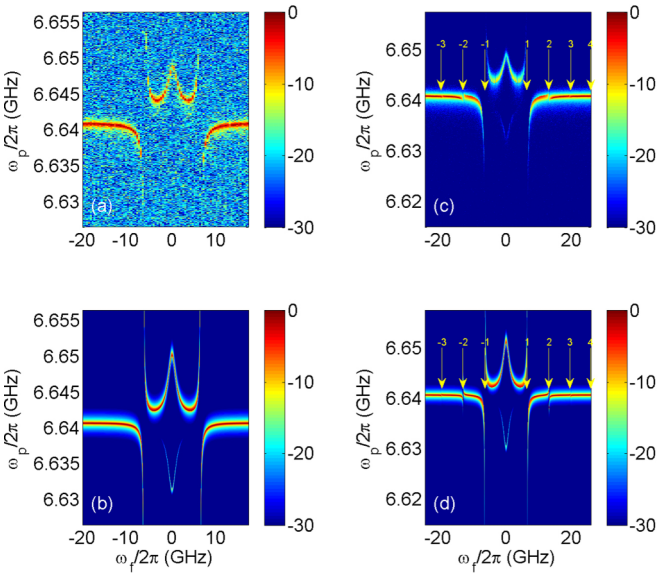

FIG. 2. The measured (a) and (c) and calculated (b) and (d) cavity transmission (in dB units) vs $\omega_f/2\pi$. For the panels on the left (a) and (b) the power injected into the cavity is -127 dBm, whereas for the panels on the right (c) and (d) the power is -112 dBm. The following parameters have been assumed in the calculation: $T = 0.023$ K, $\omega_c/2\pi = 6.6408$ GHz, $\omega_\Delta/2\pi = 1.12$ GHz, $g/2\pi = 0.274$ GHz, $\gamma_{c1}/\omega_c = 5 \times 10^{-6}$, and $\gamma_{c2} = 1.1\gamma_{c1}$. The relaxation time $T_1 = 1.2\,\mu\text{s}\,[1 + (0.45\,\text{ns})\,|\omega_f|]$ is obtained from energy relaxation measurements, and the rate $T_2^{-1} = 4.5\,\text{MHz}\,(1 + 44|\omega_f|/\omega_a)$ is obtained from Ramsey rate measurements [14]. In (a) the measured off-resonance transmission is significantly higher than the calculated one [see (b)] due to instrumental noise, which has not been taken into account in the theoretical modeling. In the region where $\Delta = \omega_c - \omega_a > 0$ two peaks are seen in the cavity transmission; the upper one corresponds to the case where the qubit mainly occupies the ground state, whereas the lower one, which is weaker, corresponds to the case where the qubit mainly occupies the first excited state. The lower peak is less visible in the data seen in (a), which was obtained at lower input power, due to reduced signal-to-noise ratio. In (c) and (d) the primary (labeled by ±1) and superharmonic (labeled by ±2, ±3 and 4) resonances are indicated by arrows.

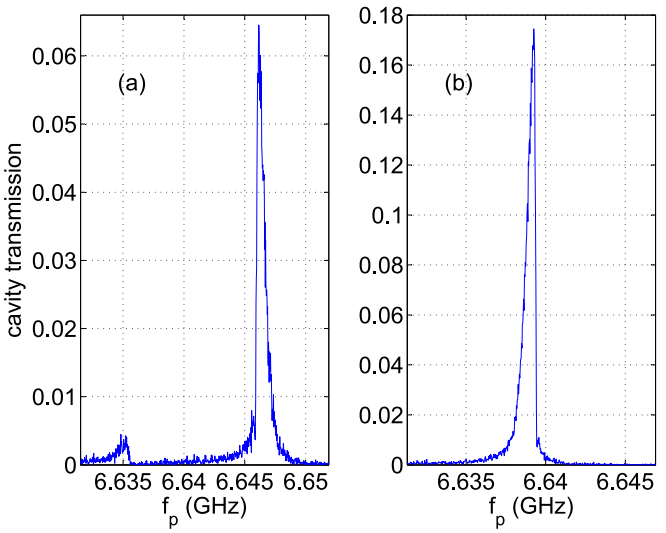

FIG. 3. Measured cavity transmission vs $f_p = \omega_p/2\pi$ cross sections of the data seen in Fig. 2(c) for (a) $\omega_f/2\pi = 1.09$ GHz and (b) $\omega_f/2\pi = 7.91$ GHz.

hardening (softening) when $\Delta_1 < 0$ ($\Delta_1 > 0$), for the case where the qubit mainly occupies its ground state. The opposite behavior is obtained when the qubit mainly occupies the first excited state. The probability for this to happen, which depends on the ratio between thermal energy and qubit energy gap, is non-negligible in the current experiment. The cases $\Delta_1 > 0$ and $\Delta_1 < 0$ are demonstrated by Figs. 3(a) and 3(b), respectively, which depict example plots of measured cavity transmission vs $f_p = \omega_p/2\pi$. In spite of the fact that many simplifying assumptions and approximations have been employed in the theoretical modeling, the comparison between the experimental results [Figs. 3(a) and 3(c)] and the theoretical predictions [Figs. 3(b) and 3(d), respectively] yields a good agreement.

It is well known that the flux qubit is expected to strongly affect the response of the cavity mode near the primary resonance, i.e., when the ratio ω_a/ω_c is tuned close to unity [see the points labeled by ±1 in Figs. 2(c) and 2(d)]. With sufficiently large driving amplitude, however, higher order nonlinear processes may give rise to SHRs, which occur near the points at which the ratio ω_a/ω_c is an integer larger than unity [see the points labeled by ±2, ±3, and 4 in Figs. 2(c) and 2(d)]. The cavity response near a SHR is theoretically evaluated in Appendix C. It is found that the same Eq. (4) can be used to describe the effect of the flux qubit on cavity response near an SHR, provided that the coupling coefficient g_1 is replaced by g_n, which is given by [see Eq. (C18)]

$$g_n = g_1 J_{1-n}\left(\frac{4g_1\omega_f E_c^{1/2}}{\omega_p\omega_\Delta}\right), \tag{6}$$

where J_l is the l'th Bessel function of the first kind, and the detuning $\Delta_1 = \omega_p - \omega_a$ is replaced by $\Delta_n = n\omega_p - \omega_a$, where at the SHR $\omega_a/\omega_c = n$. As can be seen by comparing Figs. 2(c) and 2(d), the calculated and measured cavity response near the SHRs exhibit an acceptable agreement.

IV. INTERMODULATION

In general, nonlinear cavity response is commonly employed for frequency mixing, which in turn can be used for signal amplification [40,41,45–49] and noise squeezing [42,45]. An amplifier based on flux qubits has been recently demonstrated in Ref. [50]. Here we employ the method of IMD to characterize frequency mixing. In this method, two monochromatic tones are combined and injected into the cavity: an intense pump tone at angular frequency ω_p and amplitude b_{c1}^{in}, and a weaker signal tone at angular frequency $\omega_s = \omega_p + \omega$ and amplitude c_{c1}^{in}. The cavity transmission is measured and the spectral amplitude of the output signal tone at frequency ω_s, which is labeled by $c_{c2}^{out}(\omega)$, and the spectral amplitude of the so-called idler tone at frequency $2\omega_p - \omega_s = \omega_p - \omega$, which is labeled by $c_{c2}^{out}(-\omega)$, are recorded. The corresponding signal gain $G_s = |c_{c2}^{out}(\omega)/c_{c1}^{in}|^2$ and idler gain $G_i = |c_{c2}^{out}(-\omega)/c_{c1}^{in}|^2$ are determined, and the experimental findings are compared with the theoretical predictions, which

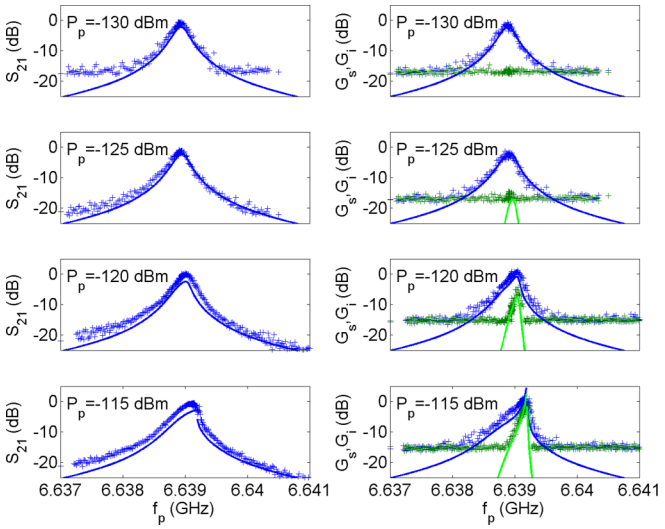

FIG. 4. Cavity transmission (panels on the left) and IMD gain (panels on the right). Experimental data are labeled by crosses whereas the solid lines represent the theoretical predictions based on Eq. (A122) for the cavity transmission S_{21}, Eq. (A127) for the signal gain G_s (blue, dark gray) and Eq. (A128) for the idler gain G_i (green, light gray). The parameters that have been employed for the calculation are listed in the caption of Fig. 2. The detuning between the signal and pump frequencies is $(\omega_s - \omega_p)/2\pi = 50\,\mathrm{kHz}$.

are based on the linearized equations of motion of the system [see Eqs. (A127) and (A128)].

The results are exhibited in Fig. 4, in which the cavity transmission S_{21} (left panels) and the signal G_s and idler G_i gains (right panels) are plotted vs pump frequency $f_p = \omega_p/2\pi$ for different values of the pump input power P_p. The magnetic flux for these measurements is set to a value for which $\omega_f/2\pi = 8.1\,\mathrm{GHz}$ and $\Delta_1/2\pi = -1.5\,\mathrm{GHz}$. The cavity transmission S_{21} is calculated according to Eq. (A122), the signal gain G_s according to Eq. (A127), and the idler gain G_i according to Eq. (A128). Relatively good agreement between data and theory is found for the results seen in Fig. 4, however, the deviation between data and theory becomes larger at higher powers. Further study is needed in order to identify the sources of discrepancy, and to improve the accuracy of the theoretical predictions accordingly.

V. SUMMARY

In summary, SHRs in the device under study have been experimentally observed. We theoretically show that a relatively simple CQED model of a system composed of two coupled elements, a single cavity mode having no intrinsic nonlinearity and a two-level system, can account for the main experimental findings. Further study will aim at expanding the range of validity of the theoretical predictions in order to account for the experimental results at higher levels of input power. Future experiments will explore the possibility of exploiting nonlinearity for improving the fidelity of qubit readout [24] and employ SHRs for generating highly correlated states of the microwave cavity field (e.g., the creation of entangled pairs of microwave photons [51] near the $n = 2$ superharmonic resonance via two-photon stimulated emission events).

ACKNOWLEDGMENTS

We thank Feyruz Kitapli and Pol Forn-Díaz for useful discussions. This research is supported by the Gerald Schwartz and Heather Reisman Foundation, NSERC, Industry Canada, CMC, CFI, Ontario MRI, and the Israeli Science Foundation.

APPENDIX A: WEAK NONLINEAR RESPONSE

1. The closed system

The Hamiltonian $\mathcal{H}_0$ of the closed system, formed by the flux qubit and the cavity mode, is taken to be given by

$$\begin{aligned}\hbar^{-1}\mathcal{H}_0 = {}& \omega_c\left(A^\dagger A + \frac{1}{2}\right) + \frac{K_c}{2}A^\dagger A^\dagger A A \\ & + \frac{\omega_f}{2}(|\curvearrowleft\rangle\langle\curvearrowleft| - |\curvearrowright\rangle\langle\curvearrowright|) \\ & + \frac{\omega_\Delta}{2}(|\curvearrowleft\rangle\langle\curvearrowright| + |\curvearrowright\rangle\langle\curvearrowleft|) \\ & - g\left(A + A^\dagger\right)(|\curvearrowleft\rangle\langle\curvearrowleft| - |\curvearrowright\rangle\langle\curvearrowright|). \end{aligned} \tag{A1}$$

The cavity mode angular resonance frequency is labeled by ω_c, K_c is the cavity mode Kerr coefficient, and A is the cavity mode annihilation operator. The coefficient $\hbar\omega_f$ is related to the externally applied magnetic flux Φ_e by

$$\frac{\hbar\omega_f}{2} = \frac{I_{cc}\Phi_0}{2\pi}\phi_e, \tag{A2}$$

where $I_{cc} = -\langle\curvearrowright|\partial\mathcal{H}_0/\partial\Phi_e|\curvearrowright\rangle$ $(-I_{cc})$ is the circulating current associated with the state $|\curvearrowright\rangle$ ($|\curvearrowleft\rangle$), $\Phi_0 = h/2e$ is the flux quantum, and the normalized applied magnetic flux ϕ_e is given by

$$\phi_e = 2\pi\left(\frac{\Phi_e}{\Phi_0} - \frac{1}{2}\right). \tag{A3}$$

The coefficient $\hbar\omega_\Delta$ is the qubit energy gap, and g is the coupling constant. The frequencies ω_f, ω_Δ, and g are assumed to be time independent.

2. Qubit energy eigenstates

The energy eigenstates of the decoupled qubit $|\pm\rangle$ are given by

$$\begin{pmatrix}|+\rangle\\ |-\rangle\end{pmatrix} = \begin{pmatrix}\cos\frac{\theta}{2} & \sin\frac{\theta}{2}\\ -\sin\frac{\theta}{2} & \cos\frac{\theta}{2}\end{pmatrix}\begin{pmatrix}|\curvearrowleft\rangle\\ |\curvearrowright\rangle\end{pmatrix}, \tag{A4}$$

where

$$\tan\theta = \frac{\omega_\Delta}{\omega_f}, \tag{A5}$$

and the corresponding eigenenergies are

$$\varepsilon_\pm = \pm\frac{\hbar\omega_a}{2}, \tag{A6}$$

where

$$\omega_a = \sqrt{\omega_f^2 + \omega_\Delta^2}. \tag{A7}$$

The following relations,

$$|\curvearrowleft\rangle\langle\curvearrowleft| - |\curvearrowright\rangle\langle\curvearrowright| = \cos\theta\ \Sigma_z - \sin\theta(\Sigma_+ + \Sigma_-), \tag{A8}$$

and

$$|\curvearrowleft\rangle\langle\curvearrowright| + |\curvearrowright\rangle\langle\curvearrowleft| = \sin\theta\ \Sigma_z + \cos\theta(\Sigma_+ + \Sigma_-), \quad \text{(A9)}$$

hold, where

$$\Sigma_z = |+\rangle\langle+| - |-\rangle\langle-|, \quad \text{(A10)}$$

$$\Sigma_+ = |+\rangle\langle-|, \quad \text{(A11)}$$

$$\Sigma_- = |-\rangle\langle+|, \quad \text{(A12)}$$

and thus the Hamiltonian $\mathcal{H}_0$ can be expressed as

$$\hbar^{-1}\mathcal{H}_0 = \omega_c\left(A^\dagger A + \frac{1}{2}\right) + \frac{K_c}{2}A^\dagger A^\dagger AA + \frac{\omega_a}{2}\Sigma_z - g(A + A^\dagger)[\cos\theta\ \Sigma_z - \sin\theta(\Sigma_+ + \Sigma_-)]. \quad \text{(A13)}$$

3. Damping

Damping is taken into account using a model containing reservoirs having dense spectrum of oscillator modes interacting with both the cavity mode and the qubit. The cavity mode is assumed to be coupled to four semi-infinite transmission lines. The first two, denoted as c1 and c2, are feedlines (or ports), which are linearly coupled to the cavity mode with coupling magnitudes γ_{c1} and γ_{c2} and coupling phases ϕ_{c1} and ϕ_{c2}, respectively, and which are employed to deliver the input and output signals. The third, denoted as c3, is linearly coupled to the cavity mode with a coupling magnitude γ_{c3} and a coupling phase ϕ_{c3}, and it is used to model linear dissipation (due to internal sources), whereas the fourth one, denoted as c4, is nonlinearly coupled to the cavity mode with a coupling magnitude γ_{c4} and a coupling phase ϕ_{c4}, and is employed to model nonlinear dissipation (due to internal sources). The qubit is assumed to be coupled to two semi-infinite transmission lines, with coupling magnitudes γ_{q1} and γ_{q2} and coupling phases ϕ_{q1} and ϕ_{q2}, respectively. While the first is employed to model energy relaxation, the second is employed to model dephasing. Note that all coupling parameters are assumed to be frequency independent. The following Bose,

$$[A, A^\dagger] = 1, \quad \text{(A14)}$$

$$[a_{cn}(\omega), a_{cm}^\dagger(\omega')] = \delta_{n,m}\delta(\omega - \omega'), \quad \text{(A15)}$$

$$[a_{qn}(\omega), a_{qm}^\dagger(\omega')] = \delta_{n,m}\delta(\omega - \omega'), \quad \text{(A16)}$$

$$[a_{cn}(\omega), a_{cm}(\omega')] = 0, \quad \text{(A17)}$$

$$[a_{qn}(\omega), a_{qm}(\omega')] = 0, \quad \text{(A18)}$$

and qubit,

$$[\Sigma_z, \Sigma_+] = 2\Sigma_+, \quad \text{(A19)}$$

$$[\Sigma_z, \Sigma_-] = -2\Sigma_-, \quad \text{(A20)}$$

$$[\Sigma_+, \Sigma_-] = \Sigma_z, \quad \text{(A21)}$$

commutation relations are assumed to hold.

The Hamiltonian $\mathcal{H}$ of the system is taken to be given by

$$\begin{aligned}\hbar^{-1}\mathcal{H} = \hbar^{-1}\mathcal{H}_0 &+ \sum_{n=1}^{4}\int d\omega\ \omega a_{cn}^\dagger(\omega)a_{cn}(\omega) \\ &+ \sum_{n=1}^{3}\sqrt{\frac{\gamma_{cn}}{\pi}}\int d\omega\ [e^{i\phi_{cn}}A^\dagger a_{cn}(\omega) + e^{-i\phi_{cn}}a_{cn}^\dagger(\omega)A] \\ &+ \sqrt{\frac{\gamma_{c4}}{2\pi}}\int d\omega\ [e^{i\phi_{c4}}A^\dagger A^\dagger a_{c4}(\omega) + e^{-i\phi_{c4}}a_{c4}^\dagger(\omega)AA] \\ &+ \sum_{n=1}^{2}\int d\omega\ \omega a_{qn}^\dagger(\omega)a_{qn}(\omega) \\ &+ \sqrt{\frac{\gamma_{q1}}{2\pi}}\int d\omega[e^{i\phi_{q1}}\Sigma_+ a_{q1}(\omega) + e^{-i\phi_{q1}}a_{q1}^\dagger(\omega)\Sigma_-] \\ &+ \sqrt{\frac{\gamma_{q2}}{4\pi}}\int d\omega[e^{i\phi_{q2}}\Sigma_z a_{q2}(\omega) + e^{-i\phi_{q2}}a_{q2}^\dagger(\omega)\Sigma_z].\end{aligned} \quad \text{(A22)}$$

4. The equations of motion

The Heisenberg equations of motion are generated according to

$$\frac{dO}{dt} = -i[O, \hbar^{-1}\mathcal{H}], \quad \text{(A23)}$$

where O is an operator and $\mathcal{H}$ is the total Hamiltonian, hence

$$\begin{aligned}\frac{dA}{dt} =& -i\omega_c A - iK_c A^\dagger AA \\ &+ ig[\cos\theta\ \Sigma_z - \sin\theta(\Sigma_+ + \Sigma_-)] \\ &- i\sum_{n=1}^{3}\sqrt{\frac{\gamma_{cn}}{\pi}}e^{i\phi_{cn}}\int d\omega\ a_{cn}(\omega) \\ &- i\sqrt{\frac{2\gamma_{c4}}{\pi}}e^{i\phi_{c4}}\int d\omega\ A^\dagger a_{c4}(\omega),\end{aligned} \quad \text{(A24)}$$

$$\begin{aligned}\frac{d\Sigma_z}{dt} =& -2ig\sin\theta\left(A + A^\dagger\right)(\Sigma_+ - \Sigma_-) - 2i\sqrt{\frac{\gamma_{q1}}{2\pi}}\int d\omega \\ &\times (e^{i\phi_{q1}}\Sigma_+ a_{q1}(\omega) - e^{-i\phi_{q1}}a_{q1}^\dagger(\omega)\Sigma_-),\end{aligned} \quad \text{(A25)}$$

$$\begin{aligned}\frac{d\Sigma_+}{dt} =& i\omega_a\Sigma_+ - ig\left(A + A^\dagger\right)(2\cos\theta\ \Sigma_+ + \sin\theta\ \Sigma_z) \\ &- i\sqrt{\frac{\gamma_{q1}}{2\pi}}\int d\omega e^{-i\phi_{q1}}a_{q1}^\dagger(\omega)\Sigma_z + i\sqrt{\frac{\gamma_{q2}}{\pi}}\int d\omega \\ &\times (e^{i\phi_{q2}}\Sigma_+ a_{q2}(\omega) + e^{-i\phi_{q2}}a_{q2}^\dagger(\omega)\Sigma_+),\end{aligned} \quad \text{(A26)}$$

$$\frac{da_{cn}(\omega)}{dt} = -i\omega a_{cn}(\omega) - i\sqrt{\frac{\gamma_{cn}}{\pi}}e^{-i\phi_{cn}}A \quad n = 1,2,3$$

$$\frac{da_{cn}(\omega)}{dt} = -i\omega a_{c4}(\omega) - i\sqrt{\frac{\gamma_{c4}}{2\pi}}e^{-i\phi_{c4}}AA \quad n = 4, \quad \text{(A27)}$$

$$\frac{da_{q1}(\omega)}{dt} = -i\omega a_{q1}(\omega) - i\sqrt{\frac{\gamma_{q1}}{2\pi}}e^{-i\phi_{q1}}\Sigma_-, \quad \text{(A28)}$$

and

$$\frac{da_{q2}(\omega)}{dt} = -i\omega a_{q2}(\omega) - i\sqrt{\frac{\gamma_{q2}}{4\pi}}e^{-i\phi_{q2}}\Sigma_z. \tag{A29}$$

5. Input-output relations

The field operator $a_{cn}(t,\omega)$ at time t can be calculated by assuming either initial value for the field operator $a_{cn}(t_0,\omega)$ at time t_0 or final value for the field operator $a_{cn}(t_1,\omega)$ at time t_1. The time t_0 is assumed to be in the distant past whereas t_1 is assumed to be in the distant future, i.e., $t_0 \ll t \ll t_1$. Time integration of (A27) using initial values at time $t_0 < t$ yields

$$\begin{aligned} a_{cn}(\omega) &= e^{-i\omega(t-t_0)}a_{cn}(t_0,\omega) - i\sqrt{\frac{\gamma_{cn}}{\pi}}e^{-i\phi_{cn}} \\ &\quad\times \int_{t_0}^{t} dt'\, e^{-i\omega(t-t')}A(t') \quad n = 1,2,3, \\ a_{cn}(\omega) &= e^{-i\omega(t-t_0)}a_{c4}(t_0,\omega) - i\sqrt{\frac{\gamma_{c4}}{2\pi}}e^{-i\phi_{c4}} \\ &\quad\times \int_{t_0}^{t} dt'\, e^{-i\omega(t-t')}A(t')A(t') \quad n = 4, \end{aligned} \tag{A30}$$

and using finite values at time $t_1 > t$ yields

$$\begin{aligned} a_{cn}(\omega) &= e^{-i\omega(t-t_1)}a_{cn}(t_1,\omega) - i\sqrt{\frac{\gamma_{cn}}{\pi}}e^{-i\phi_{cn}} \\ &\quad\times \int_{t_1}^{t} dt'\, e^{-i\omega(t-t')}A(t') \quad n = 1,2,3, \\ a_{cn}(\omega) &= e^{-i\omega(t-t_1)}a_{c4}(t_1,\omega) - i\sqrt{\frac{\gamma_{c4}}{2\pi}}e^{-i\phi_{c4}} \\ &\quad\times \int_{t_1}^{t} dt'\, e^{-i\omega(t-t')}A(t')A(t') \quad n = 4. \end{aligned} \tag{A31}$$

Integrating $a_{cn}(\omega)$ over ω and using the following relations:

$$\int_{-\infty}^{\infty} d\omega\, e^{-i\omega(t-t')} = 2\pi\delta(t-t'), \tag{A32}$$

and

$$\int_{t_c}^{t} dt'\, \delta(t-t')f(t') = \frac{1}{2}\mathrm{sgn}(t-t_c)f(t), \tag{A33}$$

where $\mathrm{sgn}(x)$ is the sign function,

$$\mathrm{sgn}(x) = \begin{cases} +1 & \text{if } x > 0 \\ -1 & \text{if } x < 0 \end{cases}, \tag{A34}$$

lead to

$$\begin{aligned} &\frac{1}{\sqrt{2\pi}}\int_{-\infty}^{\infty} d\omega\, a_{cn}(\omega) \\ &\quad = a_{cn}^{\mathrm{in}}(t) - i\sqrt{\frac{\gamma_{cn}}{2}}e^{-i\phi_{cn}}A(t) \quad n = 1,2,3 \\ &\frac{1}{\sqrt{2\pi}}\int_{-\infty}^{\infty} d\omega\, a_{cn}(\omega) \\ &\quad = a_{c4}^{\mathrm{in}}(t) - i\frac{\sqrt{\gamma_{c4}}}{2}e^{-i\phi_{c4}}A(t)A(t) \quad n = 4, \end{aligned} \tag{A35}$$

and

$$\begin{aligned} &\frac{1}{\sqrt{2\pi}}\int_{-\infty}^{\infty} d\omega\, a_{cn}(\omega) \\ &\quad = a_{cn}^{\mathrm{out}}(t) + i\sqrt{\frac{\gamma_{cn}}{2}}e^{-i\phi_{cn}}A(t) \quad n = 1,2,3 \\ &\frac{1}{\sqrt{2\pi}}\int_{-\infty}^{\infty} d\omega\, a_{cn}(\omega) \\ &\quad = a_{c4}^{\mathrm{out}}(t) + i\frac{\sqrt{\gamma_{c4}}}{2}e^{-i\phi_{c4}}A(t)A(t) \quad n = 4, \end{aligned} \tag{A36}$$

where the input operators are given by

$$a_{cn}^{\mathrm{in}}(t) = \frac{1}{\sqrt{2\pi}}\int_{-\infty}^{\infty} d\omega\, e^{-i\omega(t-t_0)}a_{cn}(t_0,\omega), \tag{A37}$$

and the output operators by

$$a_{cn}^{\mathrm{out}}(t) = \frac{1}{\sqrt{2\pi}}\int_{-\infty}^{\infty} d\omega\, e^{-i\omega(t-t_1)}a_{cn}(t_1,\omega). \tag{A38}$$

Equations (A35) and (A36) yield the following input-output relations,

$$\begin{aligned} a_{cn}^{\mathrm{out}}(t) - a_{cn}^{\mathrm{in}}(t) &= -i\sqrt{2\gamma_{cn}}e^{-i\phi_{cn}}A(t) \quad n = 1,2,3 \\ a_{cn}^{\mathrm{out}}(t) - a_{cn}^{\mathrm{in}}(t) &= -i\sqrt{\gamma_{c4}}e^{-i\phi_{c4}}A(t)A(t) \quad n = 4. \end{aligned} \tag{A39}$$

Similarly for the bath operators that are coupled to the qubit one has [see Eqs. (A28) and (A29)]

$$\frac{1}{\sqrt{2\pi}}\int_{-\infty}^{\infty} d\omega\, a_{q1}(\omega) = a_{q1}^{\mathrm{in}}(t) - i\sqrt{\frac{\gamma_{q1}}{4}}e^{-i\phi_{q1}}\Sigma_-, \tag{A40}$$

where

$$a_{q1}^{\mathrm{in}}(t) = \frac{1}{\sqrt{2\pi}}\int_{-\infty}^{\infty} d\omega\, e^{-i\omega(t-t_0)}a_{q1}(t_0,\omega), \tag{A41}$$

and

$$\frac{1}{\sqrt{2\pi}}\int_{-\infty}^{\infty} d\omega\, a_{q2}(\omega) = a_{q2}^{\mathrm{in}}(t) - i\sqrt{\frac{\gamma_{q2}}{8}}e^{-i\phi_{q2}}\Sigma_z, \tag{A42}$$

where

$$a_{q2}^{\mathrm{in}}(t) = \frac{1}{\sqrt{2\pi}}\int_{-\infty}^{\infty} d\omega\, e^{-i\omega(t-t_0)}a_{q2}(t_0,\omega). \tag{A43}$$

Thus, the equation of motion for A becomes [see Eqs. (A24) and (A35)]

$$\begin{aligned} &\frac{dA}{dt} + \left[i\omega_c + \gamma_c + (iK_c + \gamma_{c4})A^\dagger A\right]A \\ &\quad = ig[\cos\theta\ \Sigma_z - \sin\theta(\Sigma_+ + \Sigma_-)] \\ &\qquad - i\sum_{n=1}^{3}\sqrt{2\gamma_{cn}}e^{i\phi_{cn}}a_{cn}^{\mathrm{in}} - 2i\sqrt{\gamma_{c4}}e^{i\phi_{c4}}A^\dagger a_{c4}^{\mathrm{in}}, \end{aligned} \tag{A44}$$

where

$$\gamma_c = \gamma_{c1} + \gamma_{c2} + \gamma_{c3}. \tag{A45}$$

Furthermore, by making use of the following relations:

$$\Sigma_+\Sigma_- = \tfrac{1}{2}(1 + \Sigma_z), \tag{A46}$$

$$\Sigma_-\Sigma_+ = \tfrac{1}{2}(1 - \Sigma_z), \tag{A47}$$

$$\Sigma_z\Sigma_+ = -\Sigma_+\Sigma_z = \Sigma_+, \tag{A48}$$

$$\Sigma_-\Sigma_z = -\Sigma_z\Sigma_- = \Sigma_-, \tag{A49}$$

one finds that the equation of motion for Σ_z becomes [see Eqs. (A25) and (A40)]

$$\frac{d\Sigma_z}{dt} + \gamma_{q1}(1+\Sigma_z) + 2ig\sin\theta(A+A^\dagger)(\Sigma_+ - \Sigma_-) = 2i\sqrt{\gamma_{q1}}\left(-\Sigma_+ e^{i\phi_{q1}}a_{q1}^{in} + e^{-i\phi_{q1}}a_{q1}^{in\dagger}\Sigma_-\right), \tag{A50}$$

and the equation of motion for Σ_+ becomes [see Eqs. (A26) and (A42)]

$$\frac{d\Sigma_+}{dt} - i\omega_a\Sigma_+ + \left(\frac{\gamma_{q1}}{2}+\gamma_{q2}\right)\Sigma_+ + ig(A+A^\dagger)(2\cos\theta\ \Sigma_+ + \sin\theta\ \Sigma_z) = -i\sqrt{\gamma_{q1}}e^{-i\phi_{q1}}a_{q1}^{in\dagger}\Sigma_z + i\sqrt{2\gamma_{q2}}\left(\Sigma_+ e^{i\phi_{q2}}a_{q2}^{in} + e^{-i\phi_{q2}}a_{q2}^{in\dagger}\Sigma_+\right). \tag{A51}$$

6. Cavity external drive

Consider the case where a monochromatic pump tone having amplitude b_{c1}^{in} and angular frequency ω_p is injected into port 1. In a frame rotating at angular frequency ω_p the input cavity operators are expressed as

$$a_{cn}^{in} = \begin{cases} \left(b_{cn}^{in} + c_{cn}^{in}\right)e^{-i\omega_p t} & n=1 \\ c_{cn}^{in}e^{-i\omega_p t} & n=2,3,4 \end{cases}, \tag{A52}$$

the input qubit operators as

$$a_{qn}^{in} = c_{qn}^{in}e^{-i\omega_p t}, \tag{A53}$$

the output cavity operators as

$$a_{cn}^{out} = \left(b_{cn}^{out} + c_{cn}^{out}\right)e^{-i\omega_p t}, \tag{A54}$$

the cavity mode annihilation operator as

$$A = A_R e^{-i\omega_p t}, \tag{A55}$$

and the qubit operator Σ_+ as

$$\Sigma_+ = \Sigma_{+R}e^{i\omega_p t}. \tag{A56}$$

In terms of these notations Eq. (A44) becomes

$$\frac{dA_R}{dt} + [-i\Delta_{pc} + \gamma_c + (iK_c + \gamma_{c4})A_R^\dagger A_R]A_R + i\sqrt{2\gamma_{c1}}e^{i\phi_{c1}}b_{c1}^{in} - ig[\cos\theta\ \Sigma_z e^{i\omega_p t} - \sin\theta(\Sigma_{+R}e^{2i\omega_p t} + \Sigma_{+R}^\dagger)] = \mathcal{V}_A, \tag{A57}$$

where

$$\Delta_{pc} = \omega_p - \omega_c, \tag{A58}$$

and where

$$\mathcal{V}_A = -i\sum_{n=1}^{3}\sqrt{2\gamma_{cn}}e^{i\phi_{cn}}c_{cn}^{in} - 2i\sqrt{\gamma_{c4}}e^{i(\phi_{c4}+\omega_p t)}A_R^\dagger c_{c4}^{in}, \tag{A59}$$

Eq. (A50) becomes

$$\frac{d\Sigma_z}{dt} + \gamma_{q1}(1+\Sigma_z) + 2ig\sin\theta\left(A_R e^{-i\omega_p t} + A_R^\dagger e^{i\omega_p t}\right) \times (\Sigma_{+R}e^{i\omega_p t} - \Sigma_{+R}^\dagger e^{-i\omega_p t}) = \mathcal{V}_z, \tag{A60}$$

where

$$\mathcal{V}_z = 2i\sqrt{\gamma_{q1}}\left(-e^{i\phi_{q1}}\Sigma_{+R}c_{q1}^{in} + e^{-i\phi_{q1}}c_{q1}^{in\dagger}\Sigma_{+R}^\dagger\right), \tag{A61}$$

and Eq. (A51) becomes

$$\frac{d\Sigma_{+R}}{dt} + i\Delta_1\Sigma_{+R} + \left(\frac{\gamma_{q1}}{2}+\gamma_{q2}\right)\Sigma_{+R} + ig\left(A_R e^{-i\omega_p t} + A_R^\dagger e^{i\omega_p t}\right) \times (2\cos\theta\ \Sigma_{+R} + \sin\theta\ \Sigma_z e^{-i\omega_p t}) = \mathcal{V}_+, \tag{A62}$$

where

$$\Delta_1 = \omega_p - \omega_a, \tag{A63}$$

and where

$$\mathcal{V}_+ = -i\sqrt{\gamma_{q1}}e^{-i\phi_{q1}}c_{q1}^{in\dagger}\Sigma_z + i\sqrt{2\gamma_{q2}} \times \left(e^{i\phi_{q2}}\Sigma_{+R}c_{q2}^{in}e^{-i\omega_p t} + e^{-i\phi_{q2}}c_{q2}^{in\dagger}\Sigma_{+R}e^{i\omega_p t}\right). \tag{A64}$$

7. Rotating wave approximation

In the rotating wave approximation (RWA), in which rapidly oscillating terms are disregarded, the equations of motion (A57), (A60), and (A62) become

$$\frac{dA_R}{dt} + [-i\Delta_{pc} + \gamma_c + (iK_c + \gamma_{c4})A_R^\dagger A_R]A_R + i\sqrt{2\gamma_{c1}}e^{i\phi_{c1}}b_{c1}^{in} + ig_1\Sigma_{+R}^\dagger = \mathcal{V}_A, \tag{A65}$$

$$\frac{d\Sigma_z}{dt} + \gamma_{q1}(1+\Sigma_z) + 2ig_1(A_R\Sigma_{+R} - \Sigma_{+R}^\dagger A_R^\dagger) = \mathcal{V}_z, \tag{A66}$$

and

$$\frac{d\Sigma_{+R}}{dt} + i\Delta_1\Sigma_{+R} + \left(\frac{\gamma_{q1}}{2}+\gamma_{q2}\right)\Sigma_{+R} + ig_1A_R^\dagger\Sigma_z = \mathcal{V}_+, \tag{A67}$$

where

$$g_1 = g\sin\theta. \tag{A68}$$

8. Linearization

Expectation values of the operators $\mathcal{V}_A$, $\mathcal{V}_z$, and $\mathcal{V}_+$ are evaluated by assuming that bath modes are all in thermal equilibrium [43]. To first order in the damping coefficients one finds that $\langle\mathcal{V}_A\rangle$ vanishes [see Eq. (A59)] and that [see Eqs. (A61) and (A64)]

$$\langle\mathcal{V}_z\rangle = -2\gamma_{q1}n_0\langle\Sigma_z\rangle, \tag{A69}$$

$$\langle\mathcal{V}_+\rangle = -2\left(\frac{\gamma_{q1}}{2}+\gamma_{q2}\right)n_0\langle\Sigma_{+R}\rangle, \tag{A70}$$

where n_0 is the Bosonic thermal occupation number.

With the help of Eqs. (A65), (A66), (A67), (A69), and (A70) the equations of motion become

$$\frac{dA_{\mathrm{R}}}{dt} + \Theta_{\mathrm{R}} = \mathcal{F}_{\mathrm{A}}, \tag{A71}$$

$$\frac{d\Sigma_z}{dt} + \Theta_{\mathrm{z}} = \mathcal{F}_{\mathrm{z}}, \tag{A72}$$

and

$$\frac{d\Sigma_{+\mathrm{R}}}{dt} + \Theta_{+} = \mathcal{F}_{+}, \tag{A73}$$

where

$$\begin{aligned}\Theta_{\mathrm{R}}&(A_{\mathrm{R}}, A_{\mathrm{R}}^{\dagger}, \Sigma_z, \Sigma_{+\mathrm{R}}, \Sigma_{+\mathrm{R}}^{\dagger}) \\ &= [-i\Delta_{\mathrm{pc}} + \gamma_{\mathrm{c}} + (iK_{\mathrm{c}} + \gamma_{\mathrm{c4}})A_{\mathrm{R}}^{\dagger}A_{\mathrm{R}}]A_{\mathrm{R}} \\ &\quad + i\sqrt{2\gamma_{\mathrm{c1}}}e^{i\phi_{\mathrm{c1}}}b_{\mathrm{c1}}^{\mathrm{in}} + ig_1\Sigma_{+\mathrm{R}}^{\dagger},\end{aligned} \tag{A74}$$

$$\begin{aligned}\Theta_{\mathrm{z}}&(A_{\mathrm{R}}, A_{\mathrm{R}}^{\dagger}, \Sigma_z, \Sigma_{+\mathrm{R}}, \Sigma_{+\mathrm{R}}^{\dagger}) \\ &= \frac{\Sigma_z - P_0}{T_1} + 2ig_1(A_{\mathrm{R}}\Sigma_{+\mathrm{R}} - \Sigma_{+\mathrm{R}}^{\dagger}A_{\mathrm{R}}^{\dagger}),\end{aligned} \tag{A75}$$

and

$$\Theta_{+}(A_{\mathrm{R}}, A_{\mathrm{R}}^{\dagger}, \Sigma_z, \Sigma_{+\mathrm{R}}, \Sigma_{+\mathrm{R}}^{\dagger}) = \frac{\Sigma_{+\mathrm{R}}}{T_2} + i\Delta_1\Sigma_{+\mathrm{R}} + ig_1A_{\mathrm{R}}^{\dagger}\Sigma_z. \tag{A76}$$

The forcing terms $\mathcal{F}_{\mathrm{A}} = \mathcal{V}_{\mathrm{A}} - \langle\mathcal{V}_{\mathrm{A}}\rangle$, $\mathcal{F}_{\mathrm{z}} = \mathcal{V}_{\mathrm{z}} - \langle\mathcal{V}_{\mathrm{z}}\rangle$, and $\mathcal{F}_{+} = \mathcal{V}_{+} - \langle\mathcal{V}_{+}\rangle$ have a vanishing thermal expectation value. The coefficient P_0, which is given by

$$P_0 = -\frac{1}{2n_0 + 1}, \tag{A77}$$

represents the expectation value $\langle\Sigma_z\rangle$ in thermal equilibrium in the absent of external driving and when the coupling between the qubit and the cavity can be disregarded. The time T_1, which is given by

$$T_1 = -\frac{P_0}{\gamma_{\mathrm{q1}}}, \tag{A78}$$

is the qubit longitudinal relaxation time, and the time T_2, which is given by

$$T_2 = -\frac{P_0}{\frac{\gamma_{\mathrm{q1}}}{2} + \gamma_{\mathrm{q2}}} = \frac{2T_1}{1 + \frac{2\gamma_{\mathrm{q2}}}{\gamma_{\mathrm{q1}}}}, \tag{A79}$$

is the qubit transverse relaxation time.

9. Fixed points

The solution is expressed as

$$A_{\mathrm{R}} = \alpha_{\mathrm{R}} + a_{\mathrm{R}}, \tag{A80a}$$

$$\Sigma_z = P_z + \sigma_z, \tag{A80b}$$

$$\Sigma_{+\mathrm{R}} = P_{+\mathrm{R}} + \sigma_{+\mathrm{R}}, \tag{A80c}$$

where both α_{R} and $P_{+\mathrm{R}}$ are complex numbers, P_z is a real number, and the operators a_{R}, σ_z, and $\sigma_{+\mathrm{R}}$ are considered as small. Fixed points are found by solving

$$\Theta_{\mathrm{R}}(\alpha_{\mathrm{R}}, \alpha_{\mathrm{R}}^{*}, P_z, P_{+\mathrm{R}}, P_{+\mathrm{R}}^{*}) = 0, \tag{A81a}$$

$$\Theta_{\mathrm{z}}(\alpha_{\mathrm{R}}, \alpha_{\mathrm{R}}^{*}, P_z, P_{+\mathrm{R}}, P_{+\mathrm{R}}^{*}) = 0, \tag{A81b}$$

$$\Theta_{+}(\alpha_{\mathrm{R}}, \alpha_{\mathrm{R}}^{*}, P_z, P_{+\mathrm{R}}, P_{+\mathrm{R}}^{*}) = 0. \tag{A81c}$$

The solution of $\Theta_{\mathrm{z}} = \Theta_{+} = 0$ yields

$$P_{+\mathrm{R}} = -\frac{ig_1T_2\alpha_{\mathrm{R}}^{*}P_z}{1 + i\Delta_1T_2}, \tag{A82}$$

and

$$P_0 = \left(1 + \frac{4g_1^2T_1T_2|\alpha_{\mathrm{R}}|^2}{1 + \Delta_1^2T_2^2}\right)P_z, \tag{A83}$$

and thus

$$P_{+\mathrm{R}} = -\frac{ig_1T_2\alpha_{\mathrm{R}}^{*}(1 - i\Delta_1T_2)P_0}{1 + \Delta_1^2T_2^2 + 4g_1^2T_1T_2E_{\mathrm{c}}}, \tag{A84}$$

where

$$E_{\mathrm{c}} = |\alpha_{\mathrm{R}}|^2. \tag{A85}$$

Substituting into the condition $\Theta_{\mathrm{R}} = 0$ yields

$$\begin{aligned}0 =&[-i\Delta_{\mathrm{pc}} + \gamma_{\mathrm{c}} + (iK_{\mathrm{c}} + \gamma_{\mathrm{c4}})E_{\mathrm{c}} + i\Upsilon_{\mathrm{ba}}P_0]\alpha_{\mathrm{R}} \\ &+ i\sqrt{2\gamma_{\mathrm{c1}}}e^{i\phi_{\mathrm{c1}}}b_{\mathrm{c1}}^{\mathrm{in}},\end{aligned} \tag{A86}$$

where

$$\Upsilon_{\mathrm{ba}} = \frac{g_1^2T_2(i - \Delta_1T_2)}{1 + \Delta_1^2T_2^2 + 4g_1^2T_1T_2E_{\mathrm{c}}}. \tag{A87}$$

or

$$\begin{aligned}\Upsilon_{\mathrm{ba}} &= -\frac{g_1^2}{\Delta_1}\frac{1 - i\zeta_2}{1 + \zeta_2^2 + \frac{4g_1^2\zeta_2E_{\mathrm{c}}}{\Delta_1^2\zeta_1}} \\ &= -\frac{g_1^2}{\Delta_1}\frac{1 - i\zeta_2}{1 + \zeta_2^2} \\ &\quad - \frac{4ig_1^4}{\Delta_1^3}\frac{\zeta_2(i + \zeta_2)}{\zeta_1(1 + \zeta_2^2)^2}E_{\mathrm{c}} + O\left(E_{\mathrm{c}}^2\right),\end{aligned} \tag{A88}$$

where

$$\zeta_n = \frac{1}{\Delta_1T_n}, \tag{A89}$$

and where $n \in \{1,2\}$, thus to second order in $|\alpha_{\mathrm{R}}|$ Eq. (A86) can be expressed as

$$0 = (i\Omega + \Gamma)\alpha_{\mathrm{R}} + i\sqrt{2\gamma_{\mathrm{c1}}}e^{i\phi_{\mathrm{c1}}}b_{\mathrm{c1}}^{\mathrm{in}}, \tag{A90}$$

where

$$\Omega = \Omega_0 + \Omega_2E_{\mathrm{c}}, \tag{A91}$$

$$\Gamma = \Gamma_0 + \Gamma_2E_{\mathrm{c}}, \tag{A92}$$

and where

$$\Omega_0 = -\Delta_{\mathrm{pc}} - \frac{g_1^2}{\Delta_1}\frac{P_0}{1 + \zeta_2^2}, \tag{A93}$$

$$\Omega_2 = K_c + \frac{4g_1^4}{\Delta_1^3}\frac{\zeta_2 P_0}{\zeta_1\left(1+\zeta_2^2\right)^2}, \tag{A94}$$

$$\Gamma_0 = \gamma_c - \frac{g_1^2}{\Delta_1}\frac{\zeta_2 P_0}{1+\zeta_2^2}, \tag{A95}$$

$$\Gamma_2 = \gamma_{c4} + \frac{4g_1^4}{\Delta_1^3}\frac{\zeta_2^2 P_0}{\zeta_1\left(1+\zeta_2^2\right)^2}. \tag{A96}$$

Taking the module squared of Eq. (A90) leads to

$$[(\Omega_0 + \Omega_2 E_c)^2 + (\Gamma_0 + \Gamma_2 E_c)^2]E_c = S_p, \tag{A97}$$

where

$$S_p = 2\gamma_{c1}\left|b_{c1}^{in}\right|^2. \tag{A98}$$

Finding E_c by solving Eq. (A97) allows calculating α_R according to Eq. (A90), calculating P_z according to Eq. (A83), and calculating P_{+R} according to Eq. (A84).

10. Onset of bistability point

In general, for any fixed value of the driving amplitude S_p Eq. (A97) can be expressed as a relation between E_c and ω_p. When S_p is sufficiently large the response of the system becomes bistable, that is E_c becomes a multivalued function of ω_p in some range near resonance. The onset of bistability point is defined as the point for which

$$\frac{\partial \Omega_0}{\partial E_c} = 0, \tag{A99}$$

$$\frac{\partial^2 \Omega_0}{\partial E_c^2} = 0. \tag{A100}$$

By solving the above conditions one finds that the values of E_c, Ω_0, and S_p at the onset of bistability point, which are labeled as $E_{c,o}$, $\Omega_{0,o}$, and $S_{p,o}$, respectively, are given by [42]

$$E_{c,o} = \frac{2\Gamma_0}{\sqrt{3}(|\Omega_2| - \sqrt{3}\Gamma_2)}, \tag{A101}$$

$$\Omega_{0,o} = -\Gamma_0\frac{\Omega_2}{|\Omega_2|}\frac{4\Gamma_2|\Omega_2| + \sqrt{3}\left(\Omega_2^2+\Gamma_2^2\right)}{\Omega_2^2 - 3\Gamma_2^2}, \tag{A102}$$

and

$$S_{p,o} = \frac{8}{3\sqrt{3}}\frac{\Gamma_0^3(\Omega_2^2+\Gamma_2^2)}{\left(|\Omega_2| - \sqrt{3}\Gamma_2\right)^3}. \tag{A103}$$

Bistability is possible only when nonlinear damping is sufficiently small,

$$\Gamma_2 < \frac{|\Omega_2|}{\sqrt{3}}. \tag{A104}$$

11. Susceptibility

The linearized equations of motion can be expressed in a matrix form as

$$\frac{d}{dt}\begin{pmatrix} a_R \\ a_R^\dagger \\ \sigma_z \\ \sigma_{+R} \\ \sigma_{+R}^\dagger \end{pmatrix} + J\begin{pmatrix} a_R \\ a_R^\dagger \\ \sigma_z \\ \sigma_{+R} \\ \sigma_{+R}^\dagger \end{pmatrix} = \begin{pmatrix} \mathcal{F}_A \\ \mathcal{F}_A^\dagger \\ \mathcal{F}_z \\ \mathcal{F}_+ \\ \mathcal{F}_+^\dagger \end{pmatrix}, \tag{A105}$$

where

$$J = \frac{\partial(\Theta_R, \Theta_R^\dagger, \Theta_z, \Theta_+, \Theta_+^\dagger)}{\partial(A_R, A_R^\dagger, \Sigma_z, \Sigma_{+R}, \Sigma_{+R}^\dagger)} \tag{A106}$$

is the Jacobian matrix [see Eqs. (A74), (A75), and (A76)], which is evaluated at a fixed point $(\alpha_R, \alpha_R^*, P_z, P_{+R}, P_{+R}^*)$. The Jacobian matrix can be expressed as

$$J = J_0 + g_1 V, \tag{A107}$$

where J_0 is given in a block form by

$$J_0 = \left(\begin{array}{c|c} J_{0c} & 0 \\ \hline 0 & J_{0q} \end{array}\right), \tag{A108}$$

the 2×2 matrix J_{0c} is given by

$$J_{0c} = \begin{pmatrix} W & V \\ V^* & W^* \end{pmatrix}, \tag{A109}$$

and the coefficients W and V are given by

$$W = \frac{\partial \Theta_R}{\partial A_R} = -i\Delta_{pc} + \gamma_c + 2(iK_c + \gamma_{c4})E_c, \tag{A110}$$

$$V = \frac{\partial \Theta_R}{\partial A_R^\dagger} = (iK_c + \gamma_{c4})\alpha_R^2. \tag{A111}$$

The diagonal 3×3 matrix J_{0q} is given by

$$J_{0q} = \begin{pmatrix} \frac{1}{T_1} & 0 & 0 \\ 0 & \frac{1}{T_2} + i\Delta_1 & 0 \\ 0 & 0 & \frac{1}{T_2} - i\Delta_1 \end{pmatrix}, \tag{A112}$$

and the matrix V is given by

$$V = i\begin{pmatrix} 0 & 0 & 0 & 0 & 1 \\ 0 & 0 & 0 & -1 & 0 \\ 2P_{+R} & -2P_{+R}^* & 0 & 2\alpha_R & -2\alpha_R^* \\ 0 & P_z & \alpha_R^* & 0 & 0 \\ -P_z & 0 & -\alpha_R & 0 & 0 \end{pmatrix}. \tag{A113}$$

In general, the Fourier transform of a time-dependent variable or operator $O(t)$ is denoted as $O(\omega)$

$$O(t) = \frac{1}{\sqrt{2\pi}}\int_{-\infty}^{\infty} d\omega\ O(\omega)e^{-i\omega t}. \tag{A114}$$

Applying the Fourier transform to Eq. (A105) yields

$$\begin{pmatrix} a_R(\omega) \\ a_R^\dagger(-\omega) \\ \sigma_z(\omega) \\ \sigma_{+R}(\omega) \\ \sigma_{+R}^\dagger(-\omega) \end{pmatrix} = \chi(\omega)\begin{pmatrix} \mathcal{F}_A(\omega) \\ \mathcal{F}_A^\dagger(-\omega) \\ \mathcal{F}_z(\omega) \\ \mathcal{F}_+(\omega) \\ \mathcal{F}_+^\dagger(-\omega) \end{pmatrix}, \tag{A115}$$

where the susceptibility $\chi(\omega)$ is given by

$$\chi(\omega) = (J - i\omega)^{-1}. \tag{A116}$$

The matrix $\chi_0(\omega) = (J_0 - i\omega)^{-1}$ can be expressed in a block form as

$$\chi_0(\omega) = \left(\begin{array}{c|c} \chi_c(\omega) & 0 \\ \hline 0 & \chi_q(\omega) \end{array}\right), \tag{A117}$$

where the cavity block $\chi_c(\omega) = (J_{0c} - i\omega)^{-1}$ is given by

$$\chi_c(\omega) = \frac{\begin{pmatrix} W^* - i\omega & -V \\ -V^* & W - i\omega \end{pmatrix}}{(\lambda_1 - i\omega)(\lambda_2 - i\omega)}, \tag{A118}$$

λ_1 and λ_2, which are given by

$$\lambda_1 + \lambda_2 = W + W^*, \tag{A119}$$

$$\lambda_1\lambda_2 = |W|^2 - |V|^2, \tag{A120}$$

are the eigenvalues of J_{0c}, and where the qubit block $\chi_q(\omega)$ is given by

$$\chi_q(\omega) = (J_{0q} - i\omega)^{-1}. \tag{A121}$$

12. Intermodulation

In this section the output field of feedline 2 is evaluated for the case where, in addition to the pump, a monochromatic input signal is injected into feedline 1. Its amplitude $c_{c1}^{in}(\omega)$, as well as the resultant cavity mode amplitude $a_R(\omega)$ and output feedline amplitudes $c_{cn}^{out}(\omega)$ are considered as complex numbers (rather than operators). The phase ϕ_{c1} is assumed to vanish. With the help of the input-output relations given by Eq. (A39) one finds that the meanfield amplitude b_2^{out} of the output signal of feedline 2 is given by

$$b_{c2}^{out} = -i\sqrt{2\gamma_{c2}}e^{-i\phi_{c2}}\alpha_R, \tag{A122}$$

and the fluctuation amplitude $c_{c2}^{out}(\omega)$ is given by

$$c_{c2}^{out}(\omega) = -i\sqrt{2\gamma_{c2}}e^{-i\phi_{c2}}a_R(\omega). \tag{A123}$$

In terms of the cavity-cavity 2×2 block of the susceptibility matrix $\chi(\omega)$, which is denoted as $\chi_{cc}(\omega)$, the cavity amplitude $a_R(\omega)$ can be expressed as

$$\begin{pmatrix} a_R(\omega) \\ a_R^*(-\omega) \end{pmatrix} = \sqrt{2\gamma_{c1}}\chi_{cc}(\omega)\begin{pmatrix} -ic_{c1}^{in}(\omega) \\ ic_{c1}^{in*}(-\omega) \end{pmatrix}, \tag{A124}$$

and thus [see Eq. (A123)]

$$\begin{pmatrix} c_{c2}^{out}(\omega) \\ c_{c2}^{out\dagger}(-\omega) \end{pmatrix} = \mathcal{R}_{cc}\begin{pmatrix} c_{c1}^{in}(\omega) \\ -c_{c1}^{in*}(-\omega) \end{pmatrix}, \tag{A125}$$

where

$$\mathcal{R}_{cc} = 2\sqrt{\gamma_{c1}\gamma_{c2}}\begin{pmatrix} -e^{-i\phi_{c2}} & 0 \\ 0 & e^{i\phi_{c2}} \end{pmatrix}\chi_{cc}(\omega). \tag{A126}$$

The signal gain is defined by

$$G_s = \left|\frac{c_{c2}^{out}(\omega)}{c_{c1}^{in}(\omega)}\right|^2, \tag{A127}$$

and the idler gain is defined by

$$G_i = \left|\frac{c_{c2}^{out}(-\omega)}{c_{c1}^{in}(\omega)}\right|^2. \tag{A128}$$

APPENDIX B: BLOCH-SIEGERT SHIFT

Consider the case where intrinsic cavity Kerr nonlinearity can be disregarded, i.e., the case where $K_c = 0$. For that case the Hamiltonian of the closed system $\mathcal{H}_0$ (A13) can be expressed as

$$\mathcal{H}_0 = \mathcal{H}_{JC} + \mathcal{V}_{BS}, \tag{B1}$$

where $\mathcal{H}_{JC}$, which is given by

$$\hbar^{-1}\mathcal{H}_{JC} = \omega_c\left(A^\dagger A + \frac{1}{2}\right) + \frac{\omega_a}{2}\Sigma_z + g_1(A^\dagger\Sigma_- + A\Sigma_+), \tag{B2}$$

is the Jaynes-Cummings Hamiltonian, the term $\mathcal{V}_{BS}$ is given by

$$\hbar^{-1}\mathcal{V}_{BS} = g_1[A\Sigma_- + \Sigma_+A^\dagger - (A + A^\dagger)\Sigma_z\cot\theta], \tag{B3}$$

and g_1 is given by Eq. (A68). In the RWA, in which rapidly oscillating terms are disregarded, the term $\mathcal{V}_{BS}$ is ignored.

The states $|n_+\rangle$ and $|n_-\rangle$, which are given by

$$|n_+\rangle = \cos\frac{\theta_n}{2}|n,+\rangle + \sin\frac{\theta_n}{2}|n+1,-\rangle, \tag{B4}$$

$$|n_-\rangle = -\sin\frac{\theta_n}{2}|n,+\rangle + \cos\frac{\theta_n}{2}|n+1,-\rangle, \tag{B5}$$

are eigenstates of $\mathcal{H}_{JC}$ [28,29] and the following holds:

$$\mathcal{H}_{JC}|n_\pm\rangle = E_{n_\pm}|n_\pm\rangle, \tag{B6}$$

where

$$E_{n_\pm} = \hbar\left[\omega_c(n+1) \pm \frac{\omega_n}{2}\right], \tag{B7}$$

and where

$$\omega_n = \sqrt{\Delta^2 + 4g_1^2(n+1)}, \tag{B8}$$

$$\Delta = \omega_c - \omega_a, \tag{B9}$$

$$\tan\theta_n = -\frac{2g_1\sqrt{n+1}}{\Delta}. \tag{B10}$$

The ground state $|0,-\rangle$ satisfies the relation,

$$\mathcal{H}_{JC}|0,-\rangle = E_g|0,-\rangle, \tag{B11}$$

where

$$E_g = \frac{\hbar\Delta}{2} \tag{B12}$$

is the ground-state energy.

While in the RWA the term $\mathcal{V}_{BS}$ is disregarded, its effect, which gives rise to a Bloch-Siegert shift [10], is estimated below using perturbation theory. As can be seen from Eq. (B3), the perturbation $\mathcal{V}_{BS}$ is proportional to g_1. All diagonal matrix elements of $\mathcal{V}_{BS}$ in the basis of eigenstates of $\mathcal{H}_{JC}$ [see Eqs. (B4), (B5), and (B11)] vanish, and consequently the lowest nonvanishing order of the perturbation expansion is the second one. To second order in g_1 the energy of the ground state is found to be given by [see Eqs. (B8), (B9), and (B12)]

$$\hbar^{-1}E_g = \frac{\Delta}{2} + \omega_{BS,0}, \tag{B13}$$

and the energies of the excited states by

$$\hbar^{-1}E_{n_\pm} = (n+1)(\omega_c \pm \omega_{BS}) \pm \sqrt{\frac{\Delta^2}{4} + (n+1)g_1^2} + \omega_{BS,0}, \quad \text{(B14)}$$

where

$$\omega_{BS} = \frac{g_1^2}{\omega_c + \omega_a}, \quad \text{(B15)}$$

and where

$$\omega_{BS,0} = -g_1^2\left(\frac{1}{\omega_c + \omega_a} + \frac{\cot^2\theta}{\omega_c}\right). \quad \text{(B16)}$$

The following holds:

$$\hbar^{-1}(E_{n-} - E_g) = (n+1)\left(\omega_c - \omega_{BS} + \frac{g_1^2}{\Delta}\right) + O\left(g_1^4\right), \quad \text{(B17)}$$

and

$$\hbar^{-1}(E_{n+} - E_{0+}) = n\left(\omega_c + \omega_{BS} - \frac{g_1^2}{\Delta}\right) + O\left(g_1^4\right), \quad \text{(B18)}$$

thus in the linear regime and when $g_1^2/|\Delta| \ll 1$ the system has two resonance frequencies given by $\omega_c \pm \omega_{BS} \mp g_1^2/\Delta$.

APPENDIX C: SUPERHARMONIC RESONANCES

SHRs occur near the points at which the externally applied flux is tuned such that the ratio ω_a/ω_c between the qubit and cavity mode resonance frequencies becomes an integer. In the analysis below only the averaged system's response is evaluated, and thus the equations of motion can be simplified by replacing noise terms by their thermal average, and treating the operators A, Σ_z, and Σ_+ as complex numbers, which are labeled by $\alpha_p e^{-i\omega_p t}$, P_z, and P_+, respectively. In this approach Eqs. (A44), (A50), and (A51) become [see Eqs. (A69) and (A70)]

$$\frac{d\alpha_R}{dt} + [-i\Delta_{pc} + \gamma_c + (iK_c + \gamma_{c4})|\alpha_R|^2]\alpha_R = ig_1[\cot\theta P_z - (P_+ + P_+^*)]e^{i\omega_p t} - i\sqrt{2\gamma_{c1}}e^{i\phi_{c1}}b_{c1}^{in}, \quad \text{(C1)}$$

$$\frac{dP_z}{dt} + \frac{P_z - P_0}{T_1} + 2i\omega_g(P_+ - P_+^*) = 0, \quad \text{(C2)}$$

and

$$\frac{dP_+}{dt} - i\omega_a P_+ + \frac{P_+}{T_2} + i\omega_g(2\cot\theta P_+ + P_z) = 0, \quad \text{(C3)}$$

where

$$\omega_g = g_1(\alpha_R e^{-i\omega_p t} + \alpha_R^* e^{i\omega_p t}), \quad \text{(C4)}$$

and where [see Eq. (A5)]

$$\cot\theta = \frac{\omega_f}{\omega_\Delta}. \quad \text{(C5)}$$

By employing the transformation,

$$P_+ = e^{-i\theta_d}P_{d+}, \quad \text{(C6)}$$

where

$$\theta_d = \int^t dt'[2\cot\theta\omega_g(t') - \Delta_n - \omega_a],$$

and where Δ_n is a real constant (to be determined later), Eqs. (C1), (C2), and (C3) become

$$\frac{d\alpha_R}{dt} + [-i\Delta_{pc} + \gamma_c + (iK_c + \gamma_{c4})|\alpha_R|^2]\alpha_R = ig_1[\cot\theta P_z - (e^{-i\theta_d}P_{d+} + e^{i\theta_d}P_{d+}^*)]e^{i\omega_p t} - i\sqrt{2\gamma_{c1}}e^{i\phi_{c1}}b_{c1}^{in}, \quad \text{(C7)}$$

$$\frac{dP_z}{dt} + \frac{P_z - P_0}{T_1} + 2i(\zeta_g P_{d+} - \zeta_g^* P_{d+}^*) = 0, \quad \text{(C8)}$$

and

$$\frac{dP_{d+}}{dt} + \frac{P_{d+}}{T_2} + i\Delta_n P_{d+} + i\zeta_g^* P_z = 0, \quad \text{(C9)}$$

where

$$\zeta_g = \omega_g e^{-i\theta_d}. \quad \text{(C10)}$$

By employing the Jacobi-Anger expansion, which is given by

$$\exp(iz\cos\varphi) = \sum_{l=-\infty}^{\infty} i^l J_l(z)e^{il\varphi}, \quad \text{(C11)}$$

where $J_l(z)$ is the l'th Bessel function of the first kind, one finds that

$$e^{-i\theta_d} = \sum_{l=-\infty}^{\infty}\left(-\frac{\alpha_R^*}{|\alpha_R|}\right)^l J_l\left(\frac{4g_1\omega_f|\alpha_R|}{\omega_p\omega_\Delta}\right)e^{i(l\omega_p + \Delta_n + \omega_a)t}. \quad \text{(C12)}$$

Near the n'th SHR, i.e., when $\omega_a \simeq n\omega_p$, where n is an integer, the dominant term in the Jacobi-Anger expansion is the l''th one, where $l' = 1 - n$. By disregarding all other terms in the expansion, choosing the detuning frequency Δ_n to be given by

$$\Delta_n = n\omega_p - \omega_a, \quad \text{(C13)}$$

and disregarding all rapidly oscillating terms, the equations of motion (C7), (C8), and (C9) become

$$\frac{d\alpha_R}{dt} + [-i\Delta_{pc} + \gamma_c + (iK_c + \gamma_{c4})|\alpha_R|^2]\alpha_R = -\frac{i}{\alpha_R^*}\zeta_{g,n}^* P_{d+}^* - i\sqrt{2\gamma_{c1}}e^{i\phi_{c1}}b_{c1}^{in}, \quad \text{(C14)}$$

$$\frac{dP_z}{dt} + \frac{P_z - P_0}{T_1} + 2i(\zeta_{g,n}P_{d+} - \zeta_{g,n}^* P_{d+}^*) = 0, \quad \text{(C15)}$$

and

$$\frac{dP_{d+}}{dt} + \frac{P_{d+}}{T_2} + i\Delta_n P_{d+} + i\zeta_{g,n}^* P_z = 0, \quad \text{(C16)}$$

where

$$\zeta_{g,n} = \alpha_R\left(-\frac{\alpha_R^*}{|\alpha_R|}\right)^{1-n} g_n, \quad \text{(C17)}$$

and where

$$g_n = g_1 J_{1-n}\left(\frac{4g_1\omega_f|\alpha_R|}{\omega_p\omega_\Delta}\right) \quad \text{(C18)}$$

is the effective coupling coefficient of the n'th SHR.

At fixed points of the equations of motion the following holds [see Eqs. (C15) and (C16)]:

$$P_{d+} = -\frac{i\zeta^*_{g,n} T_2 P_z}{1 + i\Delta_n T_2}, \tag{C19}$$

$$P_0 = \left(1 + \frac{4T_1 T_2 |\zeta_{g,n}|^2}{1 + \Delta_n^2 T_2^2}\right) P_z, \tag{C20}$$

and thus

$$P_{d+} = -\frac{iT_2\zeta^*_{g,n}(1 - i\Delta_n T_2)P_0}{1 + \Delta_n^2 T_2^2 + 4|\zeta_{g,n}|^2 T_1 T_2}. \tag{C21}$$

Substituting into Eq. (C14) yields

$$0 = [-i\Delta_{pc} + \gamma_c + (iK_c + \gamma_{c4})E_c + i\Upsilon_{ba,n} P_0]\alpha_R + i\sqrt{2\gamma_{c1}} e^{i\phi_{c1}} b^{in}_{c1}, \tag{C22}$$

where $E_c = |\alpha_R|^2$ and where

$$\Upsilon_{ba,n} = \frac{g_n^2 T_2 (i - \Delta_n T_2)}{1 + \Delta_n^2 T_2^2 + 4g_n^2 T_1 T_2 E_c}. \tag{C23}$$

As can be seen by comparing Eqs. (C23) and (A87), the effect of the qubit on the steady-state response of the cavity mode near the n'th SHR can be taken into account in the same way as for the case of the primary resonance, provided that g_1 is substituted by g_n and Δ_1 is substituted by Δ_n.

APPENDIX D: SUPERHARMONIC RESONANCES VS MULTIPHOTON RESONANCES

The SHRs are apparently related to the so-called multiphoton resonances (MPRs), which have been observed in the response of a qubit to intense external driving when the ratio between the qubit transition frequency and the frequency of the external driving is tuned close to an integer value [52–55]. The relation between SHRs and MPRs is discussed in this appendix.

Consider the case where photon confinement by a cavity can be disregarded. The Hamiltonian of the closed system $\mathcal{H}_0$ for this case is taken to be given by [compare with Eq. (A1)]

$$\hbar^{-1}\mathcal{H}_0 = \frac{\omega_f}{2}(|\curvearrowleft\rangle\langle\curvearrowleft| - |\curvearrowright\rangle\langle\curvearrowright|) + \frac{\omega_\Delta}{2}(|\curvearrowleft\rangle\langle\curvearrowright| + |\curvearrowright\rangle\langle\curvearrowleft|). \tag{D1}$$

The externally applied flux ω_f, which was taken to be a constant in Appendix A, is now allowed to be time dependent. In terms of the operator $\sigma_+ = \zeta(t)|\curvearrowleft\rangle\langle\curvearrowright|$, where the phase factor $\zeta(t)$, which is chosen to be given by

$$\zeta(t) = \exp\left\{-i\int_0^t dt'[\omega_f(t') + \omega_d]\right\}, \tag{D2}$$

represents the transformation into a rotating frame, and where ω_d is a real constant (to be determined later), one has

$$\hbar^{-1}\mathcal{H}_0 = \frac{\omega_f}{2}\sigma_3 + \frac{\omega_\Delta}{2}[\zeta^*(t)\sigma_+ + \zeta(t)\sigma_+^\dagger], \tag{D3}$$

where $\sigma_3 = |\curvearrowleft\rangle\langle\curvearrowleft| - |\curvearrowright\rangle\langle\curvearrowright|$. The Heisenberg equations of motion that are generated by $\mathcal{H}_0$ are given by

$$\frac{d\sigma_3}{dt} = i\omega_\Delta(\zeta\sigma_+^\dagger - \zeta^*\sigma_+), \tag{D4}$$

and

$$\frac{d\sigma_+}{dt} = -i\frac{\zeta\omega_\Delta}{2}\sigma_z - i\omega_d\sigma_+. \tag{D5}$$

Consider the case of monochromatic driving at angular frequency ω_p and amplitude ω_{f1}, for which $\omega_f(t)$ is taken to be given by

$$\omega_f(t) = \omega_{f0} - \omega_{f1}\cos(\omega_p t). \tag{D6}$$

With the help of the Jacobi-Anger expansion one finds that $\zeta(t)$ can be expressed as [see Eq. (D2)]

$$\zeta(t) = \sum_{l=-\infty}^{\infty} J_l\left(\frac{\omega_{f1}}{\omega_p}\right) e^{i(l\omega_p - \omega_{f0} - \omega_d)t}. \tag{D7}$$

Near the n'th MPR, i.e., when $\omega_{f0} \simeq n\omega_p$, the detuning frequency ω_d is chosen to be given by $\omega_d = n\omega_p - \omega_{f0}$. For this case all the oscillatory terms with $l \neq n$ are disregarded in the rotating wave approximation, and thus

$$\zeta \simeq J_n\left(\frac{\omega_{f1}}{\omega_p}\right). \tag{D8}$$

In general, Eqs. (D4) and (D5) cannot be considered as Bloch equations since the eigenvectors of σ_3, i.e., the circulating current states, are not energy eigenstates. However, in the limit $\omega_\Delta \to 0$, i.e., when the circulating current states become energy eigenstates, Eqs. (D4) and (D5) can be treated as Bloch equations, and damping terms can be added accordingly,

$$\frac{d\langle\sigma_3\rangle}{dt} = i\omega_\Delta(\zeta\langle\sigma_+\rangle^* - \zeta^*\langle\sigma_+\rangle) - \frac{\langle\sigma_3\rangle - \sigma_{30}}{T_1}, \tag{D9}$$

and

$$\frac{d\langle\sigma_+\rangle}{dt} = -i\frac{\zeta\omega_\Delta}{2}\langle\sigma_z\rangle - i\omega_d\langle\sigma_+\rangle - \frac{\langle\sigma_+\rangle}{T_2}, \tag{D10}$$

where T_1 and T_2 are the longitudinal and transverse relaxation times, respectively, and where σ_{30} is the value of $\langle\sigma_3\rangle$ in thermal equilibrium (with no driving). In steady state $\langle\sigma_3\rangle$ is given by

$$\langle\sigma_3\rangle = \frac{1 + (\omega_d T_2)^2}{1 + (\omega_d T_2)^2 + (\zeta\omega_\Delta)^2 T_1 T_2}\sigma_{30}. \tag{D11}$$

To mimic the effect of a coupled cavity, the driving amplitude is taken to be given by $\omega_{f1} = 4g\sqrt{\langle N\rangle}/\hbar$, where $\langle N\rangle$ is the number of cavity photons and g is the coupling constant, and consequently Eq. (D8) becomes

$$\zeta = J_n\left(\frac{4g\sqrt{\langle N\rangle}}{\hbar\omega_p}\right). \tag{D12}$$

The above result (D12) reproduces the expression given in Refs. [52–55] for the amplitude of the n'th MPR. This result, however, is inapplicable in our experiment since the assumptions of no photon confinement and small ω_Δ are both

invalid for the case under consideration in our paper. Note that MPRs can be described in terms of Landau-Zener-Stückelberg interferometry in the so-called high barrier limit (known also as the diabatic limit) [54].

The above derivation demonstrates that no cavity is needed for the description of the underlying physics responsible for the MPRs (even though a cavity is formally introduced in the derivation given in Ref. [52]). On the other hand, the SHRs represent a truly CQED effect, which cannot be properly described without taking into account photon confinement by the cavity. It is also important to note that, in spite of an apparent similarity, the theoretically predicted behavior near a SHR significantly differs from the predicted behavior near a MPR [compare Eqs. (6) and (D12)].

[1] S. Haroche and D. Kleppner, Phys. Today **42**(1), 24 (1989).
[2] B. W. Shore and P. L. Knight, J. Mod. Opt. **40**, 1195 (1993).
[3] J. Clarke and F. K. Wilhelm, Nature (London) **453**, 1031 (2008).
[4] M. Devoret and R. Schoelkopf, Science **339**, 1169 (2013).
[5] J. You and F. Nori, Nature (London) **474**, 589 (2011).
[6] A. Blais, R.-S. Huang, A. Wallraff, S. M. Girvin, and R. J. Schoelkopf, Phys. Rev. A **69**, 062320 (2004).
[7] A. Wallraff, D. I. Schuster, A. Blais, L. Frunzio, R.-S. Huang, J. Majer, S. Kumar, S. M. Girvin, and R. J. Schoelkopf, Nature (London) **431**, 162 (2004).
[8] R. Schoelkopf and S. Girvin, Nature (London) **451**, 664 (2008).
[9] T. Niemczyk, F. Deppe, H. Huebl, E. Menzel, F. Hocke, M. Schwarz, J. Garcia-Ripoll, D. Zueco, T. Hümmer, E. Solano *et al.*, Nature Physics **6**, 772 (2010).
[10] P. Forn-Díaz, J. Lisenfeld, D. Marcos, J. J. García-Ripoll, E. Solano, C. J. P. M. Harmans, and J. E. Mooij, Phys. Rev. Lett. **105**, 237001 (2010).
[11] R. Barends, J. Kelly, A. Megrant, A. Veitia, D. Sank, E. Jeffrey, T. White, J. Mutus, A. Fowler, B. Campbell *et al.*, Nature (London) **508**, 500 (2014).
[12] J. M. Chow, J. M. Gambetta, E. Magesan, D. W. Abraham, A. W. Cross, B. Johnson, N. A. Masluk, C. A. Ryan, J. A. Smolin, S. J. Srinivasan *et al.*, Nature communications **5**, 1 (2014).
[13] D. Ristè, S. Poletto, M.-Z. Huang, A. Bruno, V. Vesterinen, O.-P. Saira, and L. DiCarlo, Nature Communications **6**, 1 (2015).
[14] J.-L. Orgiazzi, C. Deng, D. Layden, R. Marchildon, F. Kitapli, F. Shen, M. Bal, F. Ong, and A. Lupascu, Phys. Rev. B **93**, 104518 (2016).
[15] J. E. Mooij, T. P. Orlando, L. Levitov, L. Tian, C. H. V. der Wal, and S. Lloyd, Science **285**, 1036 (1999).
[16] T. P. Orlando, J. E. Mooij, L. Tian, C. H. van der Wal, L. S. Levitov, S. Lloyd, and J. J. Mazo, Phys. Rev. B **60**, 15398 (1999).
[17] A. A. Abdumalikov, Jr., O. Astafiev, Y. Nakamura, Y. A. Pashkin, and J. S. Tsai, Phys. Rev. B **78**, 180502 (2008).
[18] M. Bal, C. Deng, J.-L. Orgiazzi, F. Ong, and A. Lupascu, Nature Communications **3**, 1324 (2012).
[19] M. Jerger, S. Poletto, P. Macha, U. Hübner, E. Ilichev, and A. V. Ustinov, Appl. Phys. Lett. **101**, 042604 (2012).
[20] G. Oelsner, S. H. W. van der Ploeg, P. Macha, U. Hübner, D. Born, S. Anders, E. Il'ichev, H.-G. Meyer, M. Grajcar, S. Wünsch *et al.*, Phys. Rev. B **81**, 172505 (2010).
[21] K. Inomata, T. Yamamoto, P.-M. Billangeon, Y. Nakamura, and J. S. Tsai, Phys. Rev. B **86**, 140508 (2012).
[22] I. Serban, M. I. Dykman, and F. K. Wilhelm, Phys. Rev. A **81**, 022305 (2010).
[23] C. Laflamme and A. A. Clerk, Phys. Rev. A **83**, 033803 (2011).
[24] I. Siddiqi, R. Vijay, F. Pierre, C. M. Wilson, M. Metcalfe, C. Rigetti, L. Frunzio, and M. H. Devoret, Phys. Rev. Lett. **93**, 207002 (2004).
[25] A. Lupaşcu, E. F. C. Driessen, L. Roschier, C. J. P. M. Harmans, and J. E. Mooij, Phys. Rev. Lett. **96**, 127003 (2006).
[26] E. Boaknin, V. Manucharyan, S. Fissette, M. Metcalfe, L. Frunzio, R. Vijay, I. Siddiqi, A. Wallraff, R. Schoelkopf, and M. Devoret, arXiv:cond-mat/0702445.
[27] F. Mallet, F. R. Ong, A. Palacios-Laloy, F. Nguyen, P. Bertet, D. Vion, and D. Esteve, Nature Physics **5**, 791 (2009).
[28] M. Boissonneault, J. M. Gambetta, and A. Blais, Phys. Rev. A **77**, 060305 (2008).
[29] M. Boissonneault, J. M. Gambetta, and A. Blais, Phys. Rev. Lett. **105**, 100504 (2010).
[30] M. Boissonneault, A. C. Doherty, F. R. Ong, P. Bertet, D. Vion, D. Esteve, and A. Blais, Phys. Rev. A **89**, 022324 (2014).
[31] M. Boissonneault, A. C. Doherty, F. R. Ong, P. Bertet, D. Vion, D. Esteve, and A. Blais, Phys. Rev. A **85**, 022305 (2012).
[32] M. Boissonneault, J. M. Gambetta, and A. Blais, Phys. Rev. A **79**, 013819 (2009).
[33] M. D. Reed, L. DiCarlo, B. R. Johnson, L. Sun, D. I. Schuster, L. Frunzio, and R. J. Schoelkopf, Phys. Rev. Lett. **105**, 173601 (2010).
[34] F. R. Ong, M. Boissonneault, F. Mallet, A. C. Doherty, A. Blais, D. Vion, D. Esteve, and P. Bertet, Phys. Rev. Lett. **110**, 047001 (2013).
[35] F. R. Ong, M. Boissonneault, F. Mallet, A. Palacios-Laloy, A. Dewes, A. C. Doherty, A. Blais, P. Bertet, D. Vion, and D. Esteve, Phys. Rev. Lett. **106**, 167002 (2011).
[36] L. S. Bishop, J. Chow, J. Koch, A. Houck, M. Devoret, E. Thuneberg, S. Girvin, and R. Schoelkopf, Nature Physics **5**, 105 (2009).
[37] V. Peano and M. Thorwart, Phys. Rev. B **82**, 155129 (2010).
[38] J. Hausinger and M. Grifoni, Phys. Rev. A **83**, 030301 (2011).
[39] L. S. Bishop, E. Ginossar, and S. M. Girvin, Phys. Rev. Lett. **105**, 100505 (2010).
[40] M. Castellanos-Beltran and K. Lehnert, Appl. Phys. Lett. **91**, 083509 (2007).
[41] R. Vijay, D. H. Slichter, and I. Siddiqi, Phys. Rev. Lett. **106**, 110502 (2011).
[42] B. Yurke and E. Buks, J. Lightwave Technol. **24**, 5054 (2006).
[43] C. W. Gardiner and M. J. Collett, Phys. Rev. A **31**, 3761 (1985).
[44] S. Zaitsev, A. K. Pandey, O. Shtempluck, and E. Buks, Phys. Rev. E **84**, 046605 (2011).
[45] M. Castellanos-Beltran, K. Irwin, G. Hilton, L. Vale, and K. Lehnert, Nature Physics **4**, 929 (2008).

[46] N. Bergeal, F. Schackert, M. Metcalfe, R. Vijay, V. Manucharyan, L. Frunzio, D. Prober, R. Schoelkopf, S. Girvin, and M. Devoret, Nature (London) **465**, 64 (2010).

[47] M. Hatridge, R. Vijay, D. H. Slichter, J. Clarke, and I. Siddiqi, Phys. Rev. B **83**, 134501 (2011).

[48] B. Abdo, E. Segev, O. Shtempluck, and E. Buks, Appl. Phys. Lett. **88**, 022508 (2006).

[49] E. A. Tholen, A. Ergul, E. M. Doherty, F. M. Weber, F. Gregis, and D. B. Haviland, Appl. Phys. Lett. **90**, 253509 (2007).

[50] M. Rehák, P. Neilinger, M. Grajcar, G. Oelsner, U. Hübner, E. Il'ichev, and H.-G. Meyer, Appl. Phys. Lett. **104**, 162604 (2014).

[51] J. R. Johansson, G. Johansson, C. M. Wilson, and F. Nori, Phys. Rev. Lett. **103**, 147003 (2009).

[52] C. Cohen-Tannoudji, J. Dupont-Roc, G. Grynberg, and P. Thickstun, *Atom-Photon Interactions: Basic Processes and Applications* (Wiley Online Library, New York, 1992).

[53] Y. Nakamura, Y. A. Pashkin, and J. S. Tsai, Phys. Rev. Lett. **87**, 246601 (2001).

[54] D. M. Berns, W. D. Oliver, S. O. Valenzuela, A. V. Shytov, K. K. Berggren, L. S. Levitov, and T. P. Orlando, Phys. Rev. Lett. **97**, 150502 (2006).

[55] C. M. Wilson, T. Duty, F. Persson, M. Sandberg, G. Johansson, and P. Delsing, Phys. Rev. Lett. **98**, 257003 (2007).